JBMR®

Cathepsin K Controls Cortical Bone Formation by Degrading Periostin

Nicolas Bonnet,[1] Julia Brun,[1] Jean-Charles Rousseau,[2,3] Le T Duong,[4] and Serge L Ferrari[1]

[1]Division of Bone Diseases, Department of Internal Medicine Specialties, Geneva University Hospital & Faculty of Medicine, Geneva, Switzerland
[2]INSERM, UMR 1033, Lyon, France
[3]Université of Lyon, Villeurbanne, France
[4]Department of Bone Biology, Merck & Co., Kenilworth, NJ, USA

ABSTRACT

Although inhibitors of bone resorption concomitantly reduce bone formation because of the coupling between osteoclasts and osteoblasts, inhibition or deletion of cathepsin k (CatK) stimulates bone formation despite decreasing resorption. The molecular mechanisms responsible for this increase in bone formation, particularly at periosteal surfaces where osteoclasts are relatively poor, remain unclear. Here we show that CatK pharmacological inhibition or deletion ($Ctsk^{-/-}$ mice) potentiates mechanotransduction signals mediating cortical bone formation. We identify periostin (Postn) as a direct molecular target for degradation by CatK and show that CatK deletion increases Postn and β-catenin expression in vivo, particularly at the periosteum. In turn, Postn deletion selectively abolishes cortical, but not trabecular, bone formation in CatK-deficient mice. Taken together, these data indicate that CatK not only plays a major role in bone remodeling but also modulates modeling-based cortical bone formation by degrading periostin and thereby moderating Wnt-β-catenin signaling. These findings provide novel insights into the role of CatK on bone homeostasis and the mechanisms of increased cortical bone volume with CatK mutations and pharmacological inhibitors. © 2017 American Society for Bone and Mineral Research.

KEY WORDS: PERIOSTIN; CATHEPSIN K; MODELING; CORTICAL BONE; MECHANICAL LOADING

Introduction

Cathepsin K (CatK), a cysteine protease constitutively expressed by activated osteoclasts, digests bone matrix proteins including type I collagen, which is a key process in bone resorption.[1] CatK gene (Ctsk) mutations induce pycnodysostosis in humans, a congenital disorder characterized by deformity of the skull, maxilla and phalanges, and osteosclerosis.[2] Pycnodysostosis patients present with increased trabecular and cortical bone volume and greater cortical thickness.[3] Similarly, Ctsk deletion in mice,[4] as well as pharmacological inhibition of CatK in rabbits[5] and monkeys,[6,7] increases bone formation, including at cortical surfaces, leading to increased bone mass, improved bone structure (eg, cortical thickness), and greater bone strength. CatK inhibitors also decrease resorption by inhibiting the digestion of organic bone matrix, an effect that does not directly affect the demineralization of bone matrix or the development or survival of osteoclasts; as such, treatment with Cat K inhibitors often leads to increased numbers of resorption-deficient osteoclasts that form shallow resorption pits.[8–10] Few molecular mechanisms have been found to explain how remodeling sites direct the refilling of resorption spaces, and possible factors include a local increase in matrix-derived growth factors (IGF-1, TGF-β), which are liberated by the dissolution of the mineral phase in absence of matrix erosion[11] and/or the production of "clastokines," such as sphingosine 1 phosphate and PDGF-BB by the CatK-deficient osteoclasts.[12–15]

Intriguingly, CatK inhibitors markedly increase bone mineral density (BMD) at the hip[16] and cortical thickness at the tibia but not at the non-weight-bearing radius.[17] Similarly, bone diameter is not increased at the radius in pycnodysostosis patients.[3] Moreover, periosteal and modeling-based bone formation is increased in $Ctsk^{-/-}$ mice and in the central femur of monkeys treated with a CatK inhibitor.[4,18] These observations suggest possible interactions between mechanical forces and CatK, potentially mediated by molecules that specifically control the activation of modeling-based bone formation. How cortical bone formation is increased in absence of CatK, particularly at periosteal surfaces where it occurs primarily through de novo activation of lining cells in the absence of prior bone resorption and/or osteoclasts, remains unknown.

Osteocytes play a central role in the regulation of the bone biomechanical response, and these cells have been shown to express cathepsin K.[19–21] Central to the bone biomechanical response is the inhibition of osteocyte sclerostin expression, leading to the activation of the Wnt/β-catenin signaling pathway

in osteoblasts.[22] Another key molecule in this response and signaling activation is periostin (Postn), a matricellular protein of 90 kD secreted by osteocytes and osteoblasts.[22,23] In mice, Postn is mainly localized to the cortical compartment and its expression is essential for the periosteal bone formation mediated by Wnt-β-catenin signaling in response to mechanical loading and parathyroid hormone (PTH).[22,24–26] $Postn^{-/-}$ mice are characterized by periodontitis and low BMD, altered microstructure, and reduced cortical bone strength.[22,27] Considering the structure and function of Postn, we hypothesized that it is a potential substrate for degradation by CatK and that its levels would be increased by CatK deletion or inhibition.

In this study, we show that CatK degrades Postn in vitro and that CatK inhibition increases Postn levels and bone formation in vivo. Furthermore, the cortical bone response to loading is enhanced in $Ctsk^{-/-}$ mice in association with the increased levels of Postn both locally and systemically. In turn, the periosteal, but not trabecular, bone formation in $Ctsk^{-/-}$ mice is abolished by deletion of Postn (ie, in the background of $Postn^{-/-}$ mice).

Materials and Methods

Generation of $Ctsk^{-/-}$, $Postn^{-/-}$, and $Postn^{-/-}$ $Ctsk^{-/-}$ mice

$Postn^{-Lac\ Z}$ knock-in mice ($Postn^{-/-}$) and CatK knock-out mice ($Ctsk^{-/-}$) were generated as reported previously.[27] $Postn^{-/-}$ mice were subsequently bred with C57BL/6J mice and $Ctsk^{-/-}$ and ear punch DNA analyzed by PCR was used to identify $Ctsk$ and $Postn$ heterozygous mice. We interbred mice that were heterozygous carriers of loss-of-function $Postn$ and $Ctsk$ mutations ($Postn^{+/-}$ $Ctsk^{+/-}$ mice) to investigate the respective progeny. Mice were housed 5 per cage, maintained under standard non-barrier conditions, and had access to water and diet ad libitum (Harlan-Teklad 2019, SDS, UK). All bone phenotype analyses for non-challenged mice were performed in 12-week-old female mice ($n = 6–8$). To measure dynamic indices of bone formation, mice were injected with calcein 9 and 2 days before euthanasia. The animals were killed by cervical dislocation performed under ketamine/xylasin anesthesia, and blood was collected for serum measurements. Animal procedures were approved by the University of Geneva School of Medicine Ethical Committee and the State of Geneva Veterinarian Office.

Challenged mice

Treatment

For the pharmacological experiment C57BL6J female mice aged of 12 weeks where treated with osteoprotegerin (OPG)-Fc (4 mg/kg twice per week), alendronate (ALN, 25 μg/kg/d subcutaneously, twice a week), the cathepsin K inhibitors (L-235, 30 mg/kg twice a day) or saline (vehicle) for 4 weeks (provide by Department of Bone Biology, Merck & Co., Kenilworth, NJ, USA).

Botox experiment

Unilateral skeletal unloading was effected by Botox-induced paralysis of the quadriceps and calf muscle of one hindlimb, leaving the contralateral non-injected leg as a loaded control. $Ctsk^{-/-}$ and $Ctsk^{+/+}$ male mice (12 weeks old) were injected with Botox (19.2 μL of 2 unit/100 g, 2.5 unit/100 μL) into the left quadriceps 4 mm proximal to the patellar tendon (targeting the rectus femoris, vastus lateralis, vastus intermedius, and the vastus medialis) and the posterior compartment of the left calf (targeting the gastrocnemius, plantaris, and the soleus) ($n = 6$ mice/genotype). The Botox dose was based upon previous reports in the literature and the loss of muscle force was monitored daily by digit abduction scoring.[28,29]

In vivo axial compression

The effects of cyclic skeletal loading were assessed in C57 mice treated with antiresorptives, and in $Ctsk^{-/-}$, $Postn^{-/-}$ $Ctsk^{-/-}$, and wild-type littermate mice; all mice were 12-week-old males. A loading apparatus was specifically adapted for mouse tibial loading as previously described.[22] Custom moulded pads were placed on the longitudinal axes of the tibia to apply compression on the lower left hindlimb. The lower hindlimb was then placed on the stimulation machine between the moving pad on the proximal side (the knee) and the fixed pad on the distal side (the foot) in order to strain the tibia. The left tibia of each mouse was subjected to dynamic axial stimulation, using the following parameters: peak load = 8N, 12N, or 16N; pulse period (trapeze-shaped pulse) = 0.1 s; rest time between pulses = 10 s; full cycle frequency (pulse + rest) = 0.1 Hz. A total of 40 cycles (∼7 min) were applied per day on 3 alternate days per week for 2 weeks and euthanized 3 days later. The non-stimulated right tibia served as an internal control. Strain magnitudes were calibrated ex vivo using miniature strain gauges bound to the midshaft tibia surface, as previously reported.[30] Additional mice used for real-time qRT-PCR analyses or immunohistochemical staining were euthanized 6 hours after the last mechanical loading stimulation. As strain gauges indicated that the greatest strain levels were observed at the proximal and/or distal region of the tibia (Supplemental Fig. S1), all immunohistochemistry was performed on the proximal 1/3 of the tibia.

Bone investigation

Micro-CT scans, histomorphometry, immunohistochemistry, ELISA assay, gene expression, mechanical resistance of mouse femur or tibia were performed as described in the Supplemental Materials and Methods.[31,32] Blood from all mice was obtained just before euthanasia. After centrifugation, serum was removed and stored at –80 °C until analysis. Serum CTx (carboxy-terminal collagen cross-links) and osteocalcin were measured by ELISA assay according to manufacturer's instructions (SBA Sciences, Turku, Finland, and Biomedical Technologies Inc., Stoughton, MA, USA). Circulating levels of periostin were evaluated by an in-house assay as previously described.[33] Methodological details of Western blotting, immunocytochemistry, and ELISA analyses are in the Supplemental Materials and Methods.

Power calculation, blinding of investigators, and randomization of mouse samples

The mouse study's primary analysis was the effect of $Ctsk$ and $Postn$ inactivation on cortical bone formation rate. Power analysis indicated that 8 mice per group would provide 80% power to detect a biologically significant 1.6 SD change in bone formation rate, and therefore we aimed to use 8 mice per group for studies of basal (non-challenged) mice. For the axial tibial compression model, we used 6 mice per group because each mouse was its own control. All in vivo experiments and subsequent analyses were performed in a blinded manner. No experiments requiring randomization of sample groups were performed. No animals were excluded in our analysis.

Data analysis

The effects of pharmacological treatments were assessed by one-way ANOVA, and the effects of loading within each treatment or genotype were assessed by paired t tests. To compare the effect of treatments/genotype and the response to loading, we used a two-way ANOVA. As appropriate, post hoc testing was performed using Fisher's protected least squares difference (PLSD). Differences were considered significant at $p < 0.05$. Data are presented as mean $\pm$ SEM.

Results

Cortical bone response to axial compression increases dose dependently in Ctsk$^{-/-}$ mice

Axial compression of the tibia in wild-type mice markedly induced the expression of CatK in osteocytes as indicated by immunohistochemistry and confirmed by qRT-PCR in osteocytic fraction of tibia extracts (Fig. 1A). To investigate the role of CatK

in the cortical bone response to mechanical loading, we applied a range of forces on the tibia, from Botox-induced paralysis (–4N compared with the grounded limb) to ground reaction forces (ambulation activity 0N) to increasing axial compression (8, 12, and 16N) in adult Ctsk$^{-/-}$ mice and Ctsk$^{+/+}$ littermates. At 16N of force, the gain in BMD, bone volume/tissue volume (BV/TV), cortical bone volume (Ct.BV) as well as ultimate force and stiffness, as evaluated by the differences between the loaded and contralateral limb, were higher in Ctsk$^{-/-}$ versus Ctsk$^{+/+}$ mice (Fig. 1B–F). This improvement of bone response to loading observed in the absence of CatK became mainly significant at a force equal to or higher than 12N. In contrast, we did not see any difference between Ctsk$^{-/-}$ and Ctsk$^{+/+}$ during Botox paralysis for any of the bone parameters tested (Supplemental Fig. S2). At a similar loading force, the higher-density bones of Ctsk$^{-/-}$ mice may experience a lower strain (as shown by strain gauge data for the tibial surfaces of these mice, Fig. 1G). Thus we performed an additional experiment where we applied 1800 microstrain to both Ctsk$^{-/-}$ and Ctsk$^{+/+}$ mice, equivalent to 16N and 12N,
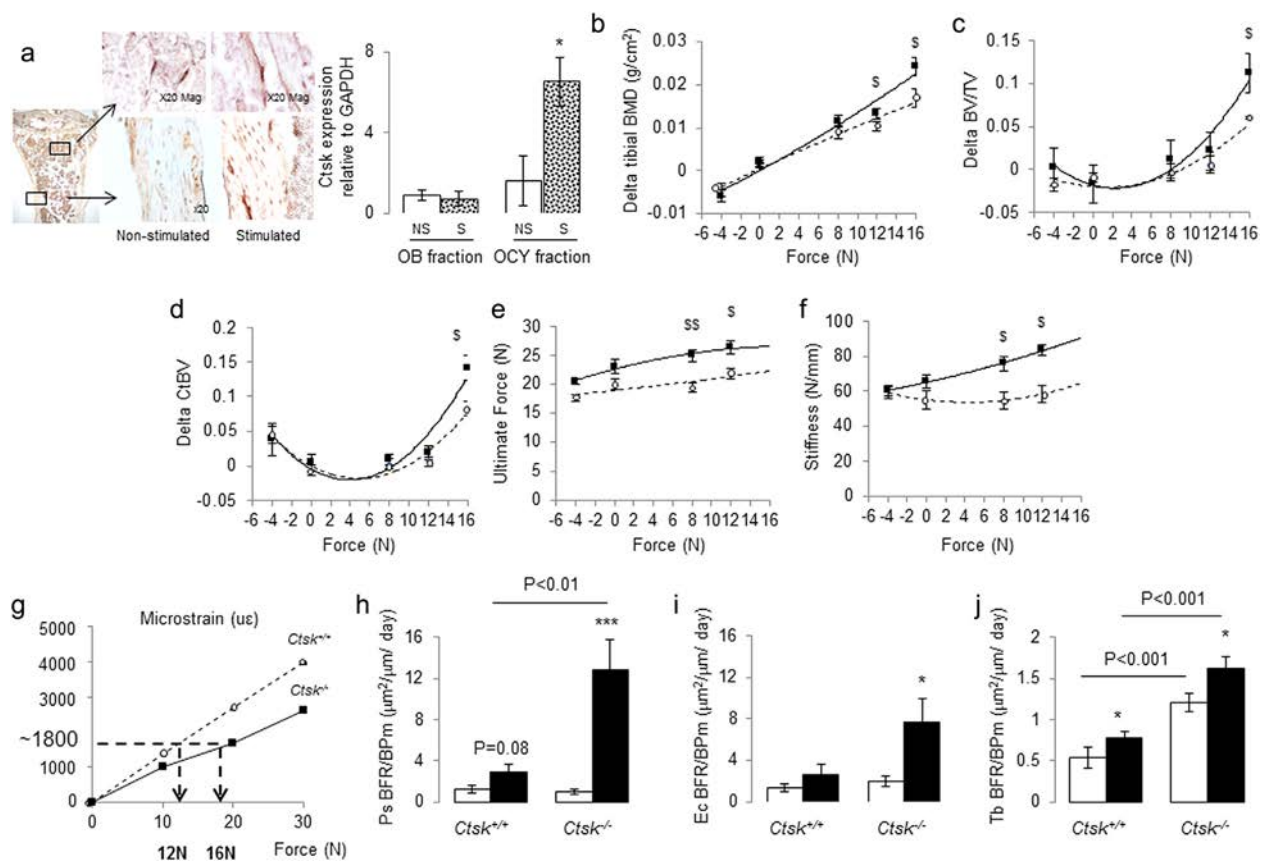

Fig. 1. Bone response to mechanical loading in Ctsk$^{-/-}$ mice and WT littermates. (A) Left panel: immunostaining of cathepsin K illustrating the increased expression in osteocytes in response to axial compression. Right panel: mRNA expression of cathepsin K in osteoblast and osteocyte fractions of tibias stimulated by axial compression (S) or non-stimulated (NS). (B–D) Left tibias were subjected to loading and the contralateral limb served as an internal control. Different levels of force were applied to Botox-immobilized limb (–4N compared with the grounded limb), ground reaction (0N), and loading by axial compression (8, 12, and 16N) in Ctsk$^{-/-}$ mice and WT littermates. (B) Delta between challenged tibia versus contralateral tibia for bone mineral density (BMD); (C) delta for trabecular bone volume per tissue volume (BV/TV) of the proximal tibia; (D) delta for cortical bone volume (Ct.BV) of the midshaft tibia. (E, F) Biomechanical properties evaluated by three-point bending of the cortical tibia. (G) Load-strain calibrations determined by strain gauge measurements on the tibia during dynamic uniaxial compression. Continuous line $=$ Ctsk$^{-/-}$; dashed line $=$ Ctsk$^{+/+}$. $^{\$}p < 0.05$, $^{\$\$}p < 0.01$ significant difference versus Ctsk$^{+/+}$ mice. (H–J) Bone formation indices in response to 1800 microstrain stimulation both in Ctsk$^{+/+}$ and Ctsk$^{-/-}$ mice, at endocortical (Ec), periosteal (Ps), and trabecular (Tb) surfaces. BFR $=$ bone formation rate; BPm $=$ bone perimeter. Bars shows mean ($\pm$SEM). Filled bars $=$ stimulated tibia; open bars $=$ non-stimulated tibia. $^{*}p < 0.05$, $^{***}p < 0.001$ significant difference vesus non-loaded tibia.

respectively, for *Ctsk*^{-/-} and *Ctsk*^{+/+} (Fig. 1*G*). Under this condition, the magnitude of the increase in periosteum bone formation rate (Ps.BFR) reached +1248% in *Ctsk*^{-/-} ($p < 0.001$ versus non-loading) versus +142% in *Ctsk*^{+/+} (ns). The increase in endocortical (Ec) BFR was also greater in *Ctsk*^{-/-}, although the difference with *Ctsk*^{+/+} mice was less prominent than at periosteal surfaces (Fig. 1*H*). In contrast, the BFR response at the trabecular surfaces was similar between *Ctsk*^{-/-} and *Ctsk*^{+/+} littermates (Fig. 1*J*).

Thus mechanical loading appears to increase the cortical bone expression of CatK (in osteocytes), and conversely, to induce larger bone formation responses in absence of CatK, specifically at cortical surfaces and most prominently at the periosteum.

CatK inhibition enhances the cortical bone response to mechanical loading

To evaluate whether the increased cortical bone response was specific to CatK inhibition or more broadly mediated by the general inhibition of osteoclasts and bone resorption, we then compared the effects of axial compression at a low force in mice treated with the CatK antagonist L-235, ALN, or OPG. When concomitantly submitted to low-amplitude axial compression, the gain in tibia Ct.BV, cortical thickness (Ct.Th), and breaking

strength was greater with L-235 (+7.9%, +9.1%, and +10.1%, respectively, versus non-loaded tibia, $p < 0.05$) compared with vehicle, ALN, or OPG-Fc (Fig. 2*A–C*). Histomorphometry showed that in response to loading, the endocortical (Ec) and trabecular (Tb) BFR at tibial midshaft were increased with vehicle and maintained with L-235, whereas ALN and OPG-Fc decreased BFR at these surfaces (Fig. 2*D*). At the periosteum (Ps), the bone forming response to loading was accentuated with L-235 (+184%) compared with vehicle (+101%, Fig. 2*E*) but absent in the ALN and OPG groups (Supplemental Table S1).

These data further indicate that CatK inhibition differs from other antiresorptives by maintaining bone formation induced by mechanical loading at remodeling surfaces while potentiating this response at modeling surfaces (periosteum). They further suggest that CatK inhibition could specifically increase the amount and/or activity of factors involved in the bone biomechanical response and expressed by non-osteoclastic cells.

CatK degrades periostin and CatK inhibition enhances periostin expression and β-catenin expression

Among the factors which expression is increased by mechanical stimulation in osteocytes and/or the periosteum, periostin appears as potential substrate for degradation by CatK. Thus we
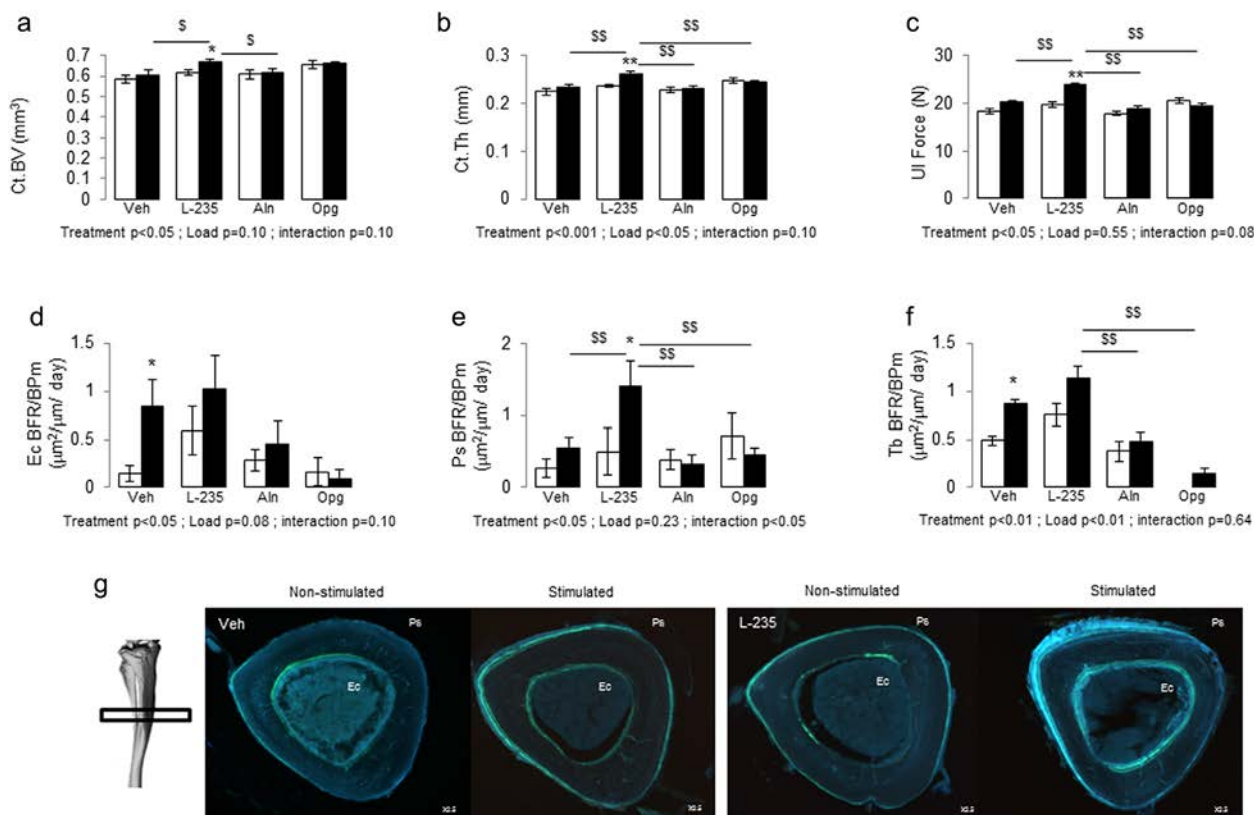

Fig. 2. Effects of the CatK inhibitor L-235 versus classical antiresorptive treatment on bone formation rate response to mechanical loading. Tibial bone parameters after 2 weeks of loading. (*A, B*) Cortical bone volume (Ct.BV) and cortical thickness (Ct.Th) at midshaft tibia. (*C*) Ultimate force evaluated by three-point bending of the cortical tibia. (*D–F*) Bone formation indices at endocortical (Ec), periosteal (Ps), and trabecular (Tb) surfaces. BFR = bone formation rate; BPm = bone perimeter. (*G*) Photomicrographs showing new bone formation with lamellar appearance in response to mechanical loading, with fluorescent calcein labels on periosteal and endosteal surfaces of the midshaft tibia. [$]$p < 0.05$ significant difference versus non-loaded tibia within the same treatment. Bars shows mean (±SEM). Filled bars = loaded tibia; open bars = non-loaded tibia.

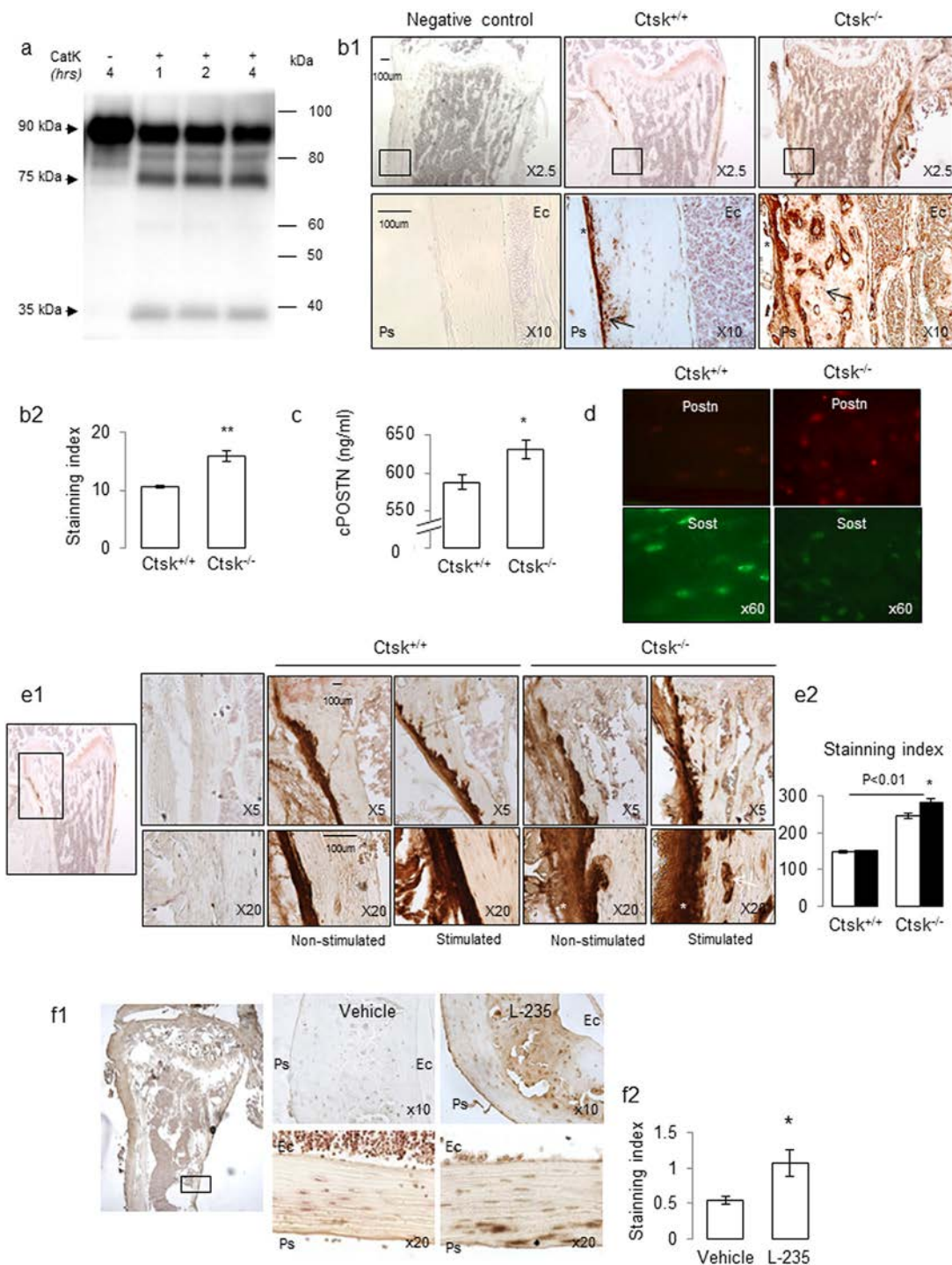**Fig. 3.** Postn is a substrate of CatK. (*A*) Human recombinant Postn incubated with CatK at 25°C for 1, 2, 3, or 12 hours. (*B1*) Immunohistochemical staining of Postn in longitudinal sections of the distal femur showing higher staining in *Ctsk*^{−/−} versus *Ctsk*^{+/+}. Note the presence of Postn in the periosteal surface (*), into osteocyte (black arrow), and endothelial cell covering intracortical pore (white arrow). (*B2*) Quantification of periostin staining was performed on longitudinal section of the 1/3 distal femur in the medial and lateral cortex. (*C*) Higher-circulating Postn levels in *Ctsk*^{−/−} versus *Ctsk*^{+/+} mice. (*D*) Double immunofluorescence of periostin (Postn) (ie, red) and sclerostin (ie, green) at midshaft femur show higher periostin and lower sclerostin level in *Ctsk*^{−/−} versus *Ctsk*^{+/+} mice. (*E1*) Immunohistochemical staining of Postn at the proximal tibia showing higher staining in response to loading, particularly in *Ctsk*^{−/−} versus *Ctsk*^{+/+}. Note the presence of Postn in periosteal surface (*) and endothelial cell covering intracortical pore (white arrow) more intense and thicker in the stimulated tibia of *Ctsk*^{−/−} versus *Ctsk*^{+/+}. (*E2*) Quantification of periostin staining was performed on longitudinal section of the 1/3 proximal tibia in the medial and lateral cortex. (*F1*) Immunohistochemical staining of β-catenin at the proximal tibia showing higher staining in L-235 versus vehicle treatment. Left panel: black box illustrates the region of interest; upper panel: cross-sectional staining of the cortex; lower panel: longitudinal section of the cortex. (*F2*) Quantification of β-catenin staining was performed on longitudinal section of the 1/3 distal femur in the medial and lateral cortex. $*p < 0.05$ significant difference versus *Ctsk*^{+/+} mice or versus vehicle treatment.

tested the in vitro proteolytic activity of recombinant human CatK in processing recombinant Postn. CatK degraded recombinant Postn by 1 hour of incubation to produce several fragments of lower molecular sizes (Fig. 3A).

Accordingly, $Ctsk^{-/-}$ mice exhibited higher periostin staining both at the periosteum and within the cortex compared with $Ctsk^{+/+}$ mice (Fig. 3B1–2), and circulating levels of periostin were higher in $Ctsk^{-/-}$ versus $Ctsk^{+/+}$ mice (Fig. 3C). Moreover, immunofluorescent levels of Postn were higher, and Sost lower, in osteocytes of the tibial cortex from $Ctsk^{-/-}$ compared with $Ctsk^{+/+}$ mice (Fig. 3D). In tibias subjected to axial compression, periostin staining was further increased in $Ctsk^{-/-}$ versus $Ctsk^{+/+}$ mice (Fig. 3E1–2). In mice treated with the CatK inhibitor L-235, the expression of canonical Wnt β-catenin pathway genes such as Axin2, c-Myc, and β-catenin (β-Ctnn1) was increased in the tibial diaphysis (respectively +23%, +86%, +25% versus Veh, $p < 0.05$, Supplemental Table S2). Increased staining for β-catenin was further observed in the tibia of mice treated with L-235 versus vehicle (Fig. 3F1–2).

Taken together with previous evidence that Postn inhibits Sost expression and activates Wnt-β-catenin signaling,[34] these observations strongly suggested that CatK inhibition potentiates the cortical bone response to loading by increasing Postn levels.

Postn deletion selectively abolishes the cortical bone effects of CatK deletion and inhibition

To directly evaluate the role of periostin on the cortical bone effects induced by deletion of CatK, $Ctsk^{-/-}$ mice were crossed with $Postn^{-/-}$ mice. As expected, $Postn^{+/+};Ctsk^{-/-}$ had higher BMD, BV/TV, and Ct.BV, whereas $Postn^{-/-};Ctsk^{+/+}$ had moderately lower femoral BMD and Ct.BV compared with $Postn^{+/+};Ctsk^{+/+}$ (Fig. 4A–C). Again $Postn^{+/+};Ctsk^{-/-}$ had higher BFR on both cortical and trabecular surfaces, confirming that bone formation was globally increased (Fig. 4D, E). In turn, Postn deletion in $Ctsk^{-/-}$ mice ($Postn^{-/-};Ctsk^{-/-}$) normalized femur BMD and Ct.BV to wild-type levels and markedly reduced cortical bone forming indices and strength compared with $Postn^{+/+};Ctsk^{-/-}$ but had no effect on trabecular BV/TV or BFR (Fig. 4C, F). Furthermore, the effects of mechanical loading on cortical bone, particularly on periosteal BFR, were suppressed in $Postn^{-/-};Ctsk^{-/-}$ mice, whereas its effects on trabecular BV/TV and BFR and, to a lesser extent, endocortical BFR remained significant (Fig. 5A–G).
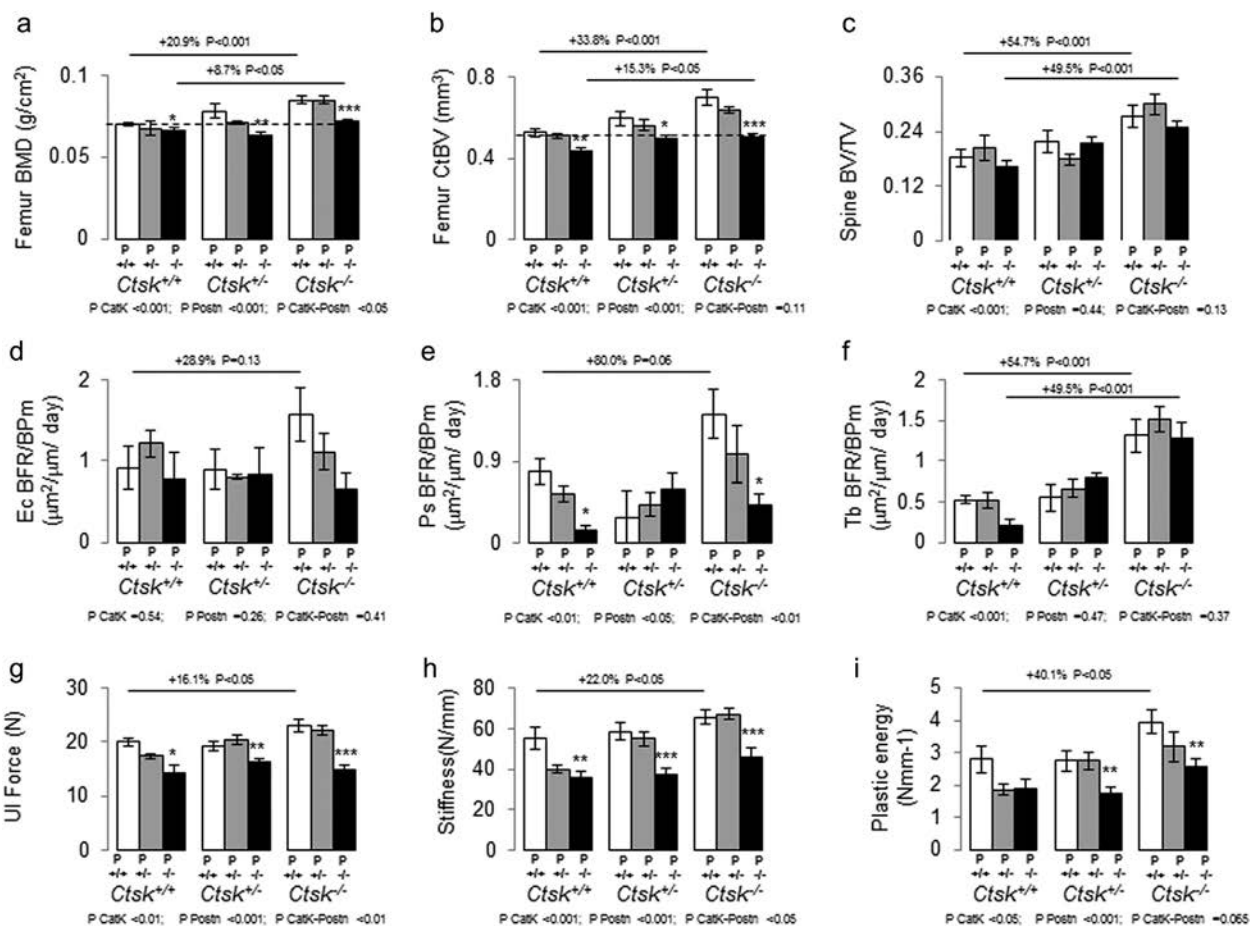

Fig. 4. Absence of Postn abolishes the cortical bone phenotype of $Ctsk^{-/-}$ mice. (A) Femur bone mineral density (BMD). (B) Cortical bone volume (Ct.BV) at midshaft femur. (C) Spine trabecular bone volume on tissue volume (BV/TV). (D–F) Bone formation indices at endocortical (Ec), periosteal (Ps), and trabecular (Tb) surfaces. BFR = bone formation rate; BPm = bone perimeter. (G–I) Biomechanical properties evaluated by three-point bending of the cortical femur. Bars shows mean (±SEM). Closed bars = mice homozygous for Postn; gray bars = mice heterozygous for Postn; open bars = mice WT for Postn. *$p < 0.05$, **$p < 0.01$, ***$p < 0.001$ significant versus $Postn^{+/+}$ mice in the respective CatK genotype.
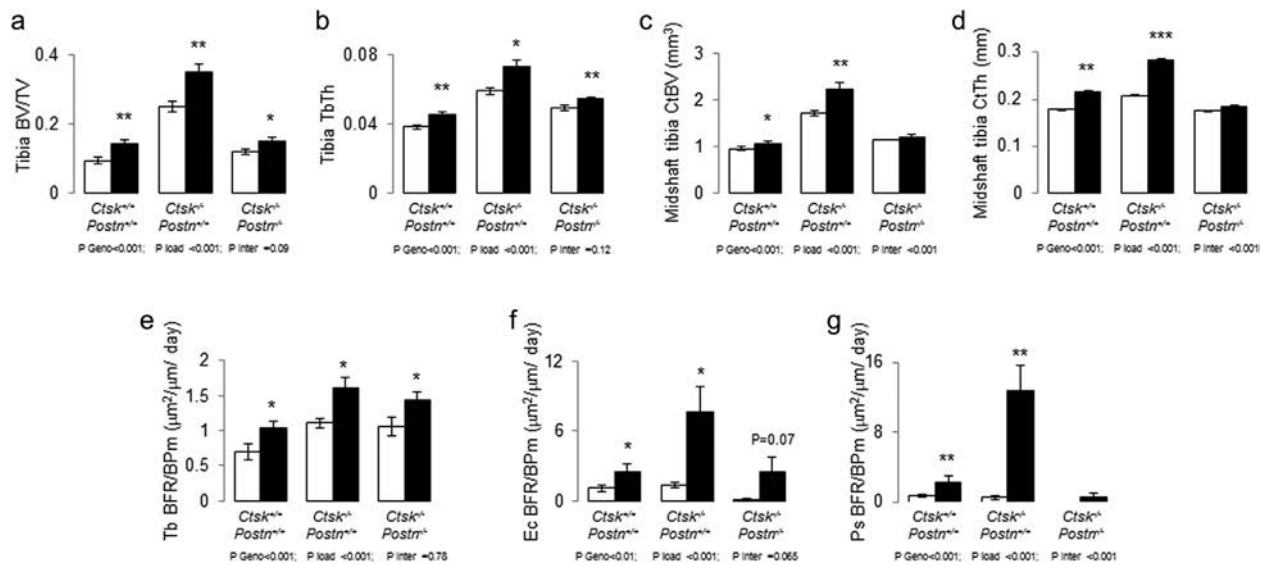
Fig. 5. Absence of Postn abolishes the cortical bone response to mechanical loading of *Ctsk*^{-/-} mice. (*A, B*) Bone volume on tissue volume (BV/TV) and trabecular thickness (Tb.Th) at the proximal tibia. (*C, D*) Cortical bone volume (Ct.BV) and cortical thickness (Ct.Th) at midshaft tibia. (*E–G*) Bone formation indices at endocortical (Ec), periosteal (Ps), and trabecular (Tb) surfaces. BFR = bone formation rate; BPm = bone perimeter. Bars show mean (±SEM). Filled bars = loaded tibia; open bars = non-loaded tibia. *$p < 0.05$, **$p < 0.01$, ***$p < 0.001$ significant versus non-loaded tibia in the respective genotype.

Similarly, the effects of the CatK antagonist L-235 on cortical structure and both periosteal and endocortical BFR were abolished in *Postn*^{-/-} mice, whereas its effects on the trabecular compartment were unaffected by Postn deletion (Supplemental Fig. S3*A–G*).

Thus increased levels of periostin resulting from CatK deletion or inhibition are selectively responsible for the increased cortical (mainly periosteal) bone formation and response to mechanical loading.

Discussion

CatK gene mutations in humans, Cat K gene deletion in mice, and pharmacological inhibitors of CatK have all shown the preservation and in some cases increased bone formation on multiple surfaces, including at the periosteum, where bone formation is largely a modeling-based osteoclast-independent process. Mechanisms for the preservation of bone formation at remodeling surfaces when CatK is absent or inhibited have been explained by an increased amount and/or activity of osteoblastic growth factors released from the demineralized bone matrix, such as IGF-1, and/or by non-resorbing osteoclasts themselves, primarily Sph1P.[14] However, the mechanisms for increased bone formation at periosteal bone surfaces under conditions of CatK inhibition remained poorly understood. By investigating the interaction of mechanical stimulation with CatK deletion and inhibition, we first showed that decreased CatK activity reduces the amount of loading required to stimulate bone formation; hence, for the same amount of strain bone formation is enhanced, indicating that CatK inhibition potentiates the skeleton's sensitivity to mechanical forces. Then by investigating the interaction between Ctsk and periostin (Postn) deletion, we demonstrated that Postn is necessary for the cortical, and particularly periosteal, bone formation induced by Ctsk inhibition.

We previously showed that the matricellular protein Postn represents an essential mediator of modeling-based bone formation in response to mechanical loading, and more broadly to anabolic stimuli, such as intermittent PTH, by its capacity to activate Wnt-β-catenin signaling both directly and through the downregulation of Sost.[22] In the present study, we demonstrated that Postn is a CatK substrate and that CatK inhibition increased Postn levels at the periosteum and in osteocytes, which induces Wnt-β-catenin activation and cortical bone formation. In turn, these experiments identify Postn as a new mechanism to explain the seemingly paradoxical observation that preventing endosteal bone remodeling by CatK inhibitors is accompanied by the activation of periosteal bone modeling.[35,36]

In *Ctsk*^{-/-} mice as well as in WT mice treated with L-235, a potent inhibitor of murine CatK,[37] BMD, microarchitecture, and strength were all improved by decreasing bone resorption but also by maintaining bone formation compared with classical antiresorptives such as OPG-Fc and alendronate. Moreover, the cortical, but not trabecular, gain in response to mechanical loading was enhanced in mice treated by L-235 compared with the classical antiresorptives. The synergistic effects of mechanical loading and CatK inhibition are attributed to the increase in cortical bone formation rate, mainly at the periosteal surfaces. Such interaction was not observed with ALN and OPG-Fc, demonstrating that it is not the inhibition of osteoclastic functions per se that is responsible for the potentiation of the bone biomechanical response but of CatK specifically. Collectively, these experimental results provide a new mechanism to potentially explain the clinical observations that CatK mutations/deletions and inhibitors prominently increase bone mineral density in weight-bearing bone. In humans, 5-year treatment with the CatK inhibitor odanacatib (ODN) increased areal bone mineral density (aBMD) at the total hip by 8.5% compared with 5% in ALN, whereas ODN and ALN had similar effects on aBMD at the distal radius, which bears less weight.[38]

In adult ovariectomized monkeys, ODN increased aBMD and strength at the femoral neck and midshaft and increased Ct.Th as well as periosteal bone formation at these bone sites.[6,7,18] It also caused greater gains in vBMD, Ct.Th, BV/TV, and estimated strength compared with ALN at key bone sites,[35] including the radius, known to be one of the most loaded sites in monkeys.[36]

Postn protein levels were higher in periosteal lining cells, osteocytes, and the circulation of Ctsk^{-/-} mice compared with WT littermates. Furthermore, mechanical loading increased Postn levels in Ctsk^{-/-} mice more than in WT mice. This increase in Postn was accompanied by an apparently decreased expression of sclerostin in osteocytes and by an activation of the Wnt-β-catenin signaling pathway. So far, there is no evidence that sclerostin is a CatK substrate, and even so, its levels in conditions of mechanical stimulation would still be expected to remain low as they are primarily driven by the downregulation of Sost gene expression. We previously demonstrated that Postn activates Wnt-β-catenin signaling in primary osteoblastic cell cultures and in TOPGAL reporter mice that uses a ß-galactosidase reporter gene (LacZ) under the control of multimerized TCF binding sites. We also reported that Postn activates integrin-mediated signaling (AKT/PKB and FAK) in osteoblasts, thereby promoting cell adhesion and motility by activation of the actin/myosin contractile machinery.[39,40] Subsequently, Postn inhibits GSK3β, a main regulator of the Wnt-β-catenin axis via PIP3 and/or AKT.[41] Altogether, these experiments indicate that CatK inhibitors interacting with mechanical forces increase Postn levels and induce cortical bone formation, most prominently at modeling-based surfaces (periosteum), through the activation of the Wnt-β-catenin pathway (Fig. 6). In contrast, Postn signaling does not appear to play a major role in the increase of trabecular bone volume by CatK inhibitors, which may actually depend on the production of other coupling factors in the bone remodeling units.[14,15,42] Although it is likely that several other proteins, including IGF-1 and BMP-2,[11] are elevated with CatK inhibition, our results in periostin null mice demonstrate that among all possible substrates, periostin is necessary and sufficient to explain the increased mechanosensitivity of the skeleton when CatK activity is reduced.

By using a global knock-out for CatK, one of the potential limitations of our study is that we cannot determine specifically which CatK-expressing cells, namely osteoclasts, osteocytes, or other bone cells, are mostly responsible for periostin degradation and the inhibition of modeling-based bone formation at the periosteum. Osteoclasts have been observed in the periosteum, where periostin is also expressed, both in mice and humans,[43–45] however at very low levels and only in specific regions (metaphysis) and/or during growth or aging in humans. However, we did not specifically observe periosteal osteoclasts at the midshaft in our experiment, suggesting osteoclasts were not a key source of CatK for periostin degradation. Because periostin is expressed in osteoblasts and osteocytes, where CatK expression has also been reported,[46] and considering our observation that mechanical stimuli increase CatK expression as well as periostin in these cells, we postulate that periostin degradation by CatK occurs primarily as a paracrine mechanism by these cells. In our study, we used male or female mice indifferently for the genetic and pharmacologic experiments
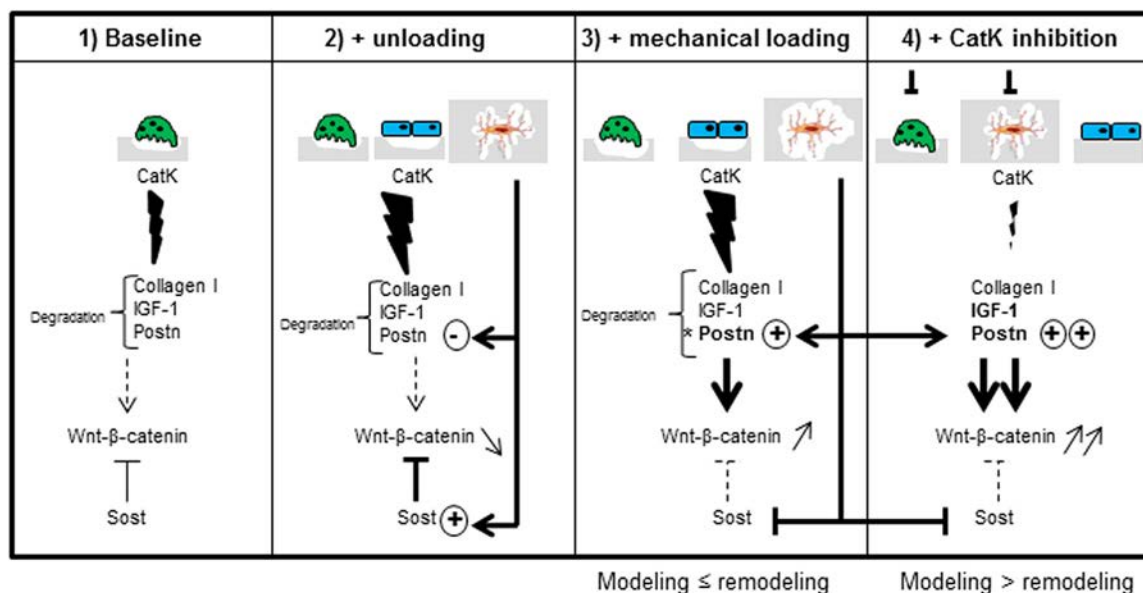

Fig. 6. Schematic representation of the role of Postn on Wnt-β-catenin on the bone remodeling/modeling ratio in response to mechanical loading and CatK inhibition. 1) Activated osteoclasts (green cells) produce CatK, which degrades collagen and non-collagen bone proteins at the trabecular and cortical surface, including Postn that normally stimulates Wnt-β-catenin signaling, whereas sclerostin (Sost) inhibits Wnt-β-catenin. 2) Unloading induces decreases in Postn and increases Sost expression in osteocytes, hence decreasing Wnt-β-catenin and bone formation; because of the initial decrease of periostin substrate inhibition of cathepsin K did not prevent bone formation decrease in response to Botox. 3) Mechanical loading induces Postn expression and downregulates Sost in osteocytes, hence increasing Wnt-β-catenin signaling, which enhances modeling-based bone formation; in addition, loading increases cathepsin K in osteoblast lining cells (blue cells) and osteocytes (orange cells), which degrades bone matrix all around the lacunae, including a part of periostin. *Limited increase through degradation by CatK. 4) CatK inhibition increases Postn levels, further potentiated by mechanical loading, hence increasing Wnt-β-catenin signaling and modeling-based bone formation, while bone remodeling is maintained or reduced.

and found concordant results independent of sex. These results are in accordance with Pennypacker and colleagues, who reported that the bone phenotype of $Ctsk^{-/-}$ mice is similar in males and females.[4]

Serum Postn has been shown to decrease with age and to be correlated with cortical bone microarchitecture both in animals and in humans.[47] Cortical bone, which represents more than 80% of skeletal mass, provides important mechanical support.[48,49] Despite the fact that longitudinal growth through an endochondral mechanism has been extensively studied, mechanisms that regulate bone width particularly in the mature skeleton are less known. Our findings may implicate CatK activity in the acceleration of bone remodeling after the menopause as a central mechanism that not only degrades endosteal bone structures but also limits the compensatory increase in modeling-based bone formation (through periostin degradation) that would normally occur at the periosteum as a result of the increased strain imparted to the structurally weaker bones.

Taken together, these data indicate that CatK not only plays a major role in bone remodeling but also can modulate the modeling-based cortical response to mechanical forces by degrading periostin and thereby moderating Wnt-β-catenin signaling. These findings provide novel insights into the role of CatK on bone homeostasis and the mechanisms for increased cortical bone volume in pycnodysostosis and in response to CatK inhibitors.

Disclosures

All authors state that they have no conflicts of interest.

Acknowledgments

References

1. Søe K, Merrild DM, Delaissé JM. Steering the osteoclast through the demineralization-collagenolysis balance. Bone. 2013;56(1):191–8.

2. Motyckova G, Fisher DE. Pycnodysostosis: role and regulation of cathepsin K in osteoclast function and human disease. Curr Mol Med. 2002;2(5):407–21.

3. Schilling AF, Mülhausen C, Lehmann W, et al. High bone mineral density in pycnodysostotic patients with a novel mutation in the propeptide of cathepsin K. Osteoporos Int. 2007;18(5):659–69.

4. Pennypacker B, Shea M, Liu Q, et al. Bone density, strength, and formation in adult cathepsin K (-/-) mice. Bone. 2009;44(2):199–207.

5. Pennypacker BL, Duong le T, Cusick TE, et al. Cathepsin K inhibitors prevent bone loss in estrogen-deficient rabbits. J Bone Miner Res. 2011;26(2):252–62.

6. Cusick T, Chen CM, Pennypacker BL, et al. Odanacatib treatment increases hip bone mass and cortical thickness by preserving endocortical bone formation and stimulating periosteal bone formation in the ovariectomized adult rhesus monkey. J Bone Miner Res. 2012;27:524–37.

7. Jerome C, Missbach M, Gamse R. Balicatib, a cathepsin K inhibitor, stimulates periosteal bone formation in monkeys. Osteoporos Int. 2012;23(1):339–49.

8. Leung P, Pickarski M, Zhuo Y, Masarachia PJ, Duong LT. The effects of the cathepsin K inhibitor odanacatib on osteoclastic bone resorption and vesicular trafficking. Bone. 2011;49(4):623–35.

9. Bone HG, McClung MR, Roux C, et al. Odanacatib, a cathepsin-K inhibitor for osteoporosis: a two-year study in postmenopausal women with low bone density. J Bone Miner Res. 2010;25(5):937–47.

10. Rachner TD, Khosla S, Hofbauer LC. Osteoporosis: now and the future. Lancet. 2011;377(9773):1276–87.

11. Fuller K, Lawrence KM, Ross JL, et al. Cathepsin K inhibitors prevent matrix-derived growth factor degradation by human osteoclasts. Bone. 2008;42(1):200–11.

12. Zhao C, Irie N, Takada Y, et al. Bidirectional ephrinB2-EphB4 signaling controls bone homeostasis. Cell Metab. 2006;4(2):111–21.

13. Nakahama K. Cellular communications in bone homeostasis and repair. Cell Mol Life Sci. 2010;67(23):4001–9.

14. Cao X. Targeting osteoclast-osteoblast communication. Nat Med. 2011;17(11):1344–6.

15. Xie H, Cui Z, Wang L, et al. PDGF-BB secreted by preosteoclasts induces angiogenesis during coupling with osteogenesis. Nat Med. 2014;20(11):1270–8.

16. Engelke K, Nagase S, Fuerst T, et al. The effect of the cathepsin K inhibitor ONO-5334 on trabecular and cortical bone in postmenopausal osteoporosis: the OCEAN study. J Bone Miner Res. 2014;29(3):629–38.

17. Cheung AM, Majumdar S, Brixen K, et al. Effects of odanacatib on the radius and tibia of postmenopausal women: improvements in bone geometry, microarchitecture, and estimated bone strength. J Bone Miner Res. 2014;29(8):1786–94.

18. Pennypacker BL, Chen CM, Zheng H, et al. Inhibition of cathepsin K increases modeling-based bone formation, and improves cortical dimension and strength in adult ovariectomized monkeys. J Bone Miner Res. 2014;29(8):1847–58.

19. Prideaux M, Schutz C, Wijenayaka AR, et al. Isolation of osteocytes from human trabecular bone. Bone. 2016 88:64–72.

20. Qing H, Ardeshirpour L, Pajevic PD, et al. Demonstration of osteocytic perilacunar/canalicular remodeling in mice during lactation. J Bone Miner Res. 2012;27(5):1018–29.

21. Kogawa M, Wijenayaka AR, Ormsby RT, et al. Sclerostin regulates release of bone mineral by osteocytes by induction of carbonic anhydrase 2. J Bone Miner Res. 2013;28(12):2436–48.

22. Bonnet N, Standley KN, Bianchi EN, et al. The matricellular protein Periostin is required for Sclerostin inhibition and the anabolic response to mechanical loading and physical activity. J Biol Chem. 2009;284(51):35939–50.

23. Rani S, Barbe MF, Barr AE, Litvin J. Periostin-like-factor and Periostin in an animal model of work-related musculoskeletal disorder. Bone. 2009;44(3):502–12.

24. Rhee Y, Allen MR, Condon K, et al. PTH receptor signaling in osteocytes governs periosteal bone formation and intracortical remodeling. J Bone Miner Res. 2011;26(5):1035–46.

25. Bonnet N, Ferrari SL. Periostin expression mediates Sost inhibition and cortical bone anabolic response to PTH. Bone. 2010;47(Suppl):s46.

26. Gerbaix M, Vico L, Ferrari SL, Bonnet N. Periostin expression contributes to cortical bone loss during unloading. Bone. 2015;71:94–100.

27. Rios H, Koushik SV, Wang H, et al. Periostin null mice exhibit dwarfism, incisor enamel defects, and an early-onset periodontal disease-like phenotype. Mol Cell Biol. 2005;25(24):11131–44.

28. Chappard D, Chennebault A, Moreau M, Legrand E, Audran M, Basle MF. Texture analysis of X-ray radiographs is a more reliable descriptor

of bone loss than mineral content in a rat model of localized disuse induced by the Clostridium botulinum toxin. Bone. 2001;28(1):72–9.

29. Warner SE, Sanford DA, Becker BA, Bain SD, Srinivasan S, Gross TS. Botox induced muscle paralysis rapidly degrades bone. Bone. 2006;38(2):257–64.

30. Stadelmann VA, Hocke J, Verhelle J, et al. 3D strain map of axially loaded mouse tibia: a numerical analysis validated by experimental measurements. Comput Methods Biomech Biomed Engin. 2008; 12(1):95–100.

31. Bouxsein ML, Boyd SK, Christiansen BA, Guldberg RE, Jepsen KJ, Müller R. Guidelines for assessment of bone microstructure in rodents using micro-computed tomography. J Bone Miner Res. 2010;25(7):1468–86.

32. Dempster DW, Compston JE, Drezner MK, et al. Standardized nomenclature, symbols, and units for bone histomorphometry: a2012 update of the report of the ASBMR Histomorphometry Nomenclature Committee. J Bone Miner Res. 2013;28(1):2–17.

33. Contié S, Voorzanger-Rousselot N, Litvin J, et al. Development of a new ELISA for serum periostin: evaluation of growth-related changes and bisphosphonate treatment in mice. Calcif Tissue Int. 2010;87(4):341–50.

34. Bonnet N, Conway SJ, Ferrari SL. Regulation of beta catenin signaling and parathyroid hormone anabolic effects in bone by the matricellular protein periostin. Proc Natl Acad Sci U S A. 2012; 109(37):15048–53.

35. Williams DS, McCracken PJ, Purcell M, et al. Effect of odanacatib on bone turnover markers, bone density and geometry of the spine and hip of ovariectomized monkeys: a head-to-head comparison with alendronate. Bone. 2013;56(2):489–96.

36. Jayakar RY, Cabal A, Szumiloski J, et al. Evaluation of high-resolution peripheral quantitative computed tomography, finite element analysis and biomechanical testing in a pre-clinical model of osteoporosis: a study with odanacatib treatment in the ovariecto-mized adult rhesus monkey. Bone. 2012;50(6):1379–88.

37. Duong LT, Wesolowski GA, Leung P, Oballa R, Pickarski M. Efficacy of a cathepsin K inhibitor in a preclinical model for prevention and treatment of breast cancer bone metastasis. Mol Cancer Ther. 2014;13(12):2898–909.

38. Langdahl B, Binkley N, Bone H, et al. Odanacatib in the treatment of postmenopausal women with low bone mineral density: five years of continued therapy in a phase 2 study. J Bone Miner Res. 2012;27(11):2251–8.

39. Gillan L, Matei D, Fishman DA, Gerbin CS, Karlan BY, Chang DD. Periostin secreted by epithelial ovarian carcinoma is a ligand for alpha(V)beta(3) and alpha(V)beta(5) integrins and promotes cell motility. Cancer Res. 2002;62(18):5358–64.

40. Shimazaki M, Nakamura K, Kii I, et al. Periostin is essential for cardiac healing after acute myocardial infarction. J Exp Med. 2008;205(2): 295–303.

41. Morra L, Moch H. Periostin expression and epithelial-mesenchymal transition in cancer: a review and an update. Virchows Arch. 2011; 459(5):465–75.

42. Lotinun S, Kiviranta R, Matsubara T, et al. Osteoclast-specific cathepsin K deletion stimulates S1P-dependent bone formation. J Clin Invest. 2013;123(2):666–81.

43. Balena R, Shih MS, Parfitt AM. Bone resorption and formation on the periosteal envelope of the ilium: a histomorphometric study in healthy women. J Bone Miner Res. 1992;7(12):1475–82.

44. Bliziotes M, Sibonga JD, Turner RT, Orwoll E. Periosteal remodeling at the femoral neck in nonhuman primates. J Bone Miner Res. 2006; 21(7):1060–7.

45. Frey SP, Jansen H, Doht S, Filgueira L, Zellweger R. Immunohisto-chemical and molecular characterization of the human periosteum. Sci World J. 2013;341078.

46. Mandelin J, Hukkanen M, Li TF, et al. Human osteoblasts produce cathepsin K. Bone. 2006;38(6):769–77.

47. Bonnet N, Biver E, Durosier C, Chevalley T, Rizzoli R, Ferrari S. Additive genetic effects on circulating periostin contribute to the heritability of bone microstructure. J Clin Endocrinol Metab. 2015;100(7):E1014–21.

48. Zebaze RM, Ghasem-Zadeh A, Bohte A, et al. Intracortical remodelling and porosity in the distal radius and post-mortem femurs of women: a cross-sectional study. Lancet. 2010;375(9727): 1729–36.

49. Seeman E. Periosteal bone formation—a neglected determinant of bone strength. N Engl J Med. 2003;349(4):320–3.